

Article

Fuzzy-Based Adaptive Dynamic Surface Control for a Type of Uncertain Nonlinear System with Unknown Actuator Faults

Xiongfeng Deng ^{1,2,*} and Jiakai Wang ³¹ School of Electrical Engineering, Anhui Polytechnic University, Wuhu 241000, China² Key Laboratory of Advanced Perception and Intelligent Control of High-End Equipment, Ministry of Education, Anhui Polytechnic University, Wuhu 241000, China³ College of Engineering & Science, University of Detroit Mercy, Detroit, MI 48221, USA; wangji12@udmercy.edu

* Correspondence: dengxiongfeng@ahpu.edu.cn

Abstract: In this paper, the adaptive control problem of a type of uncertain nonlinear system is addressed. The system discussed includes unknown nonlinear functions, uncertain nonlinear dynamics, and unknown actuator faults. Based on the fuzzy logic systems and dynamic surface control technique, an adaptive fuzzy control law is designed to solve the tracking control problem. In control law design, fuzzy logic systems are utilized to approximate uncertain nonlinear functions, and with the help of the dynamic surface control technique, the problem of the “explosion of complexity” can be overcome. Through stability analysis, it is confirmed that all of the signals in the closed-loop system are semi-global bounded, and the convergence of the tracking error to the specified small neighborhood of the origin can be ensured by adjusting the control law parameters. Finally, the effectiveness of the proposed control law is verified by simulation examples.

**Citation:** Deng, X.; Wang, J.

Fuzzy-Based Adaptive Dynamic Surface Control for a Type of Uncertain Nonlinear System with Unknown Actuator Faults.

Mathematics **2022**, *10*, 1624. <https://doi.org/10.3390/math10101624>

Academic Editors: Jan Awrejcewicz, José M. Vega, Hari Mohan Srivastava, Ying-Cheng Lai, Hamed Farokhi, Roman Starosta and Luigi Fortuna

Received: 18 April 2022

Accepted: 7 May 2022

Published: 10 May 2022

Publisher’s Note: MDPI stays neutral with regard to jurisdictional claims in published maps and institutional affiliations.



Copyright: © 2022 by the authors. Licensee MDPI, Basel, Switzerland. This article is an open access article distributed under the terms and conditions of the Creative Commons Attribution (CC BY) license (<https://creativecommons.org/licenses/by/4.0/>).

Keywords: nonlinear system; fuzzy logic systems; dynamic surface control; actuator fault**MSC:** 93C10; 93C40; 93C42

1. Introduction

In the past decades, the adaptive control problems of nonlinear systems have received extensive attention in unmanned aerial vehicle systems, robotic systems, manipulator systems, and industrial control systems; see [1–5] and the references therein. To obtain better control performance, model predictive control [1], sliding mode control [4], state feedback control [6], and adaptive backstepping control [3,7] have been proposed. However, in several practical systems, there are usually complex nonlinear characteristics, such as uncertain nonlinear dynamics [2,8], strict-feedback nonlinear dynamics [7,9], nonaffine nonlinear dynamics [10], and pure-feedback nonlinear dynamics [11]. In the face of these complex nonlinear dynamics, how to design control laws and carry out the related theoretical analysis has always been a hot topic.

Due to the existence of nonlinear dynamics, some analysis approaches, such as the linearization method [12], the mean value theorem [13], the satisfaction of the Lipschitz condition [14], and the neural networks/fuzzy logic systems approximator [4,6,15–17] have been widely utilized. However, the methods considered in [12–14] usually need to meet some assumptions, such as the differentiable condition, the matching condition, or the growth condition, which are too strict for the analysis of practical nonlinear systems. Hence, the backstepping control technique is considered by some researchers for the control problem of nonlinear systems.

As an effective analytical method, the backstepping control technique is usually combined with various control methods to solve the control problems of various uncertain nonlinear systems. In [18,19], the adaptive backstepping control law was developed for

the fractional-order nonlinear system and the strict-feedback nonlinear system, respectively. Owing to the application of design control laws, perfect tracking results can be achieved. In [20–22], the adaptive finite-time command filtered backstepping control law was designed to solve the tracking problem of uncertain nonlinear systems. In view of the approximation characteristics of neural networks and fuzzy logic systems, adaptive backstepping control approaches with neural networks or fuzzy logic systems are widely applied. In [23], the adaptive backstepping control schemes with fuzzy logic systems are proposed to solve the fault-tolerant control problem of nonlinear systems. In addition, by using the adaptive backstepping control law with neural networks, the tracking control problem of nonlinear systems with time-delay and unknown input saturation was achieved in [24], and the fault-tolerant control for a class of fractional-order nonlinear systems with actuator faults is discussed in [25].

In spite of the many control strategies with the backstepping control method that have been proposed and adopted in the existing literature, the problem of the “explosion of complexity” needs to be considered when using the backstepping control technique to design control laws. Given that virtual control laws and nonlinear functions need to be repeatedly differentiated in the backstepping recursive design, the complexity of the controller increases significantly with the increase of the order of the systems, especially for high-order nonlinear systems. For this purpose, the dynamic surface control approach has been considered by several researchers and does not require obtaining the derivative of virtual control laws in the previous step. Based on the advantage of the dynamic surface control method, the control problems of nonlinear systems with all kinds of constraints were designed in [26–28]. In [29,30], dynamic surface control laws with fuzzy logic systems were studied for the tracking problems of nonlinear systems with input saturation and time-varying output constraints and output delay, respectively. For the control problem of nonlinear large-scale systems with time delay, a better control effect was obtained by using the designed adaptive decentralized fuzzy dynamic surface control law in [31,32], and in [33,34], the dynamic surface control laws with neural networks for the control problems of interconnected systems and uncertain nonlinear systems were considered, respectively. Moreover, the neuro-fuzzy-based adaptive dynamic surface control strategy was investigated in [35].

In several practical systems, due to the influence and limitation of various factors, actuators may suffer from failure. For this, in [16,36], the adaptive fuzzy control laws for the nonlinear interconnected systems and stochastic nonlinear high-order multiagent systems were designed, where the coupled denial-of-service attacks and actuator faults and nonaffine nonlinear faults were considered. In [37], a set-invariance adaptive dynamic surface control scheme was designed for uncertain large-scale nonlinear input-saturated systems. Under the designed adaptive fuzzy tracking control scheme, the tracking problems of uncertain nonlinear systems with dead-zone input were analyzed in [9,10,38]. Moreover, the backlash failure [20], the stuck failure [39], and input quantization [40] were also considered by researchers. Nevertheless, it is worth noting that the occurrence of actuator faults is accidental, which makes the parameters of actuator faults unknown. Therefore, it is worth studying the control problems of systems with actuator faults.

Motivated by the above-mentioned research, this paper discusses the adaptive tracking control problem of a type of uncertain nonlinear system with unknown actuator faults. The main contributions of this paper are summarized as follows:

- (1) The adaptive fuzzy dynamic surface control scheme is designed for the uncertain nonlinear system in the presence of actuator faults, where the fault occurring in the system is assumed to be unknown. Compared with the references [41,42], the fault model considered in this paper is more general;
- (2) Different from references [18,19], the problem of the “explosion of complexity” can be overcome owing to the introduction of the dynamic surface control technique, and the derivation of nonlinear terms in the backstepping recursive design is eliminated.

In addition, fuzzy logic systems are used to approximate the unknown nonlinear dynamics, which effectively reduces the difficulty of the control law design;

- (3) The effectiveness of the control law designed in this paper is proved by theoretical analysis. By adjusting the design parameters, it is also proved that all of the signals in the closed-loop system are semi-global bounded, and the tracking error converges to the specified small neighborhood of the origin.

The rest of this paper is organized as follows. In Section 2, the problem description and preliminaries are provided. In Section 3, the main results for the adaptive fuzzy dynamic surface control for the uncertain nonlinear system with unknown actuator faults are discussed. Thereafter, the stability analysis and simulation analysis are given in Sections 4 and 5, respectively. Finally, the conclusions are briefly drawn in Section 6.

Notation 1. Throughout this paper, $|\cdot|$ denotes the absolute value of real number or the distance of real space R . $(\cdot)^T$ denotes the transposition of a vector. $\tanh(\cdot)$ denotes the hyperbolic tangent function. $\lambda_{\max}(X)$ represents the largest eigenvalue of the matrix X . H_{iM} stands for the maximum value of function $H_i(\cdot)$. $\text{diag}(\cdot)$ is the diagonal matrix. $\bar{x}_i(t) = [x_1(t), x_2(t), \dots, x_i(t)]^T$ represents the states vector. $\hat{\theta}$ represents the estimation of the ideal parameter vector θ^* . ψ_{id} represents the i th virtual control law.

2. Problem Description and Preliminaries

2.1. System Description

Consider a class of uncertain nonlinear system with unknown actuator faults as the following form:

$$\begin{cases} \dot{x}_i(t) = x_{i+1}(t) + f_i(\bar{x}_i(t)), i = 1, 2, \dots, n - 1 \\ \dot{x}_n(t) = v(t) + f_n(\bar{x}_n(t)) + \Delta_n(\bar{x}_n(t)) \\ y = x_1 \end{cases} \tag{1}$$

where $\bar{x}_i(t) = [x_1(t), x_2(t), \dots, x_i(t)]^T (i = 1, 2, \dots, n)$, $x_1(t), \dots, x_n(t)$ and $v(t)$ represents the states of system and actual control input, respectively; $f_i(\bar{x}_i(t)) (i = 1, 2, \dots, n)$ is an unknown smooth nonlinear function; $\Delta_n(\bar{x}_n(t))$ is an uncertain nonlinear dynamic.

In this paper, the model of the actuator fault is considered as the actuator’s loss of effectiveness and bias signal, which is described as:

$$v(t) = \rho u(t) + f_0(t), \forall t > t_1 \tag{2}$$

where ρ denotes the actuator health condition and satisfies $0 < \rho_0 \leq \rho \leq 1$, ρ_0 is an unknown positive constant; $u(t)$ is the control input to be designed; $f_0(t)$ denotes the bounded time-varying bias signal and occurs at any unknown instant t_1 , then there exists an unknown positive constant f_0^* and satisfies $|f_0(t)| \leq f_0^*$, for $\forall t \geq t_1$. Clearly, $\rho = 1$ indicates that the system is fault-free, and $\rho_0 \leq \rho < 1$ indicates that the actuator’s partial loss of effort.

The control objective of this paper is to develop an adaptive control law $u(t)$ for the system (1) by combing the fuzzy logic systems and dynamic surface control technique such that the system output y tracks the desired reference trajectory y_d under the unknown actuator fault, and all of the signals in the closed-loop system are bounded.

Note 1: For practical complex systems, there are usually complex nonlinear dynamics, and their accurate mathematical model is often difficult to obtain. Thus, the smooth nonlinear functions $f_i(\bar{x}_i(t)) (i = 1, 2, \dots, n)$ in system (1) are considered as the unknown nonlinear dynamics. In addition, in terms of possible external disturbances, unmolded dynamics, and modeling errors, they are uniformly considered and defined as the uncertain nonlinear dynamic $\Delta_n(\bar{x}_n(t))$ in system (1).

Note 2: For the fault model of the system, the main consideration in this paper is the actuator loss of effectiveness and bias signal. Based on the change of actuator health condition ρ and time-varying bias signal $f_0(t)$, the fault types in different situations can be realized. Compared with these single fault types, such as input saturation fault [37], dead-zone

input [10,38], the backlash failure [20], the stuck failure [39], and input quantization [40], the fault model considered in this paper is more general.

2.2. Fuzzy Logic Systems

A fuzzy logic system usually consists of four parts, that is, the fuzzifier, the fuzzy rule base, the fuzzy inference engine, and the defuzzifier [38]. The fuzzy rule base consists of the following of “if-then” rules:

$$R^l: \text{ If } x_1 \text{ is } F_1^l, \dots, \text{ and } x_n \text{ is } F_n^l, \text{ then } h \text{ is } G^l, \quad l = 1, 2, \dots, M.$$

where $x = [x_1, x_2, \dots, x_n]^T$ and h are the fuzzy logic system’s input and output, respectively; M is the number of “if-then” rules; $F_1^l, F_2^l, \dots, F_n^l$ and G^l are fuzzy sets for linguistic variables x_1, x_2, \dots, x_n , and h , respectively.

According to the description in reference [38], the fuzzy logic system can be expressed as:

$$h(x) = \frac{\sum_{l=1}^M \bar{h}_l \prod_{i=1}^n \mu_{F_i^l}(x_i)}{\sum_{l=1}^M \left[\prod_{i=1}^n \mu_{F_i^l}(x_i) \right]} \tag{3}$$

where $\bar{h}_l = \max_{h \in R} \mu_{G^l}(h)$, $\mu_{F_i^l}(x_i)$ and $\mu_{G^l}(y)$ are membership functions of fuzzy sets F_i^l and G^l , respectively.

Defining the fuzzy basis function as:

$$\zeta_l(x) = \frac{\prod_{i=1}^n \mu_{F_i^l}(x_i)}{\sum_{l=1}^M \left[\prod_{i=1}^n \mu_{F_i^l}(x_i) \right]}, \quad l = 1, 2, \dots, M \tag{4}$$

Let $\theta^T = [\bar{h}_1, \bar{h}_2, \dots, \bar{h}_M] = [\theta_1, \theta_2, \dots, \theta_M]$ and $\zeta(x) = [\zeta_1(x), \zeta_2(x), \dots, \zeta_M(x)]^T$, then (3) is rewritten as:

$$h(x) = \theta^T \zeta(x) \tag{5}$$

Lemma 1 [38]. For any continuous function $f(x)$ defined on a compact set Ω_x and any given positive constant ε , there exists a fuzzy logic system (5) such that:

$$\sup_{x \in \Omega_x} |f(x) - h(x)| = |f(x) - \theta^T \zeta(x)| \leq \varepsilon \tag{6}$$

where ε is the approximation accuracy and can be arbitrarily small.

According to [10], let θ^* be the ideal parameter vector of the fuzzy logic system, then we have:

$$\theta^* = \operatorname{argmin}_{\theta \in \Omega_\theta} \sup_{x \in \Omega_x} |f(x) - \theta^T \zeta(x)| \tag{7}$$

where Ω_θ and Ω_x are the compact set for θ and x .

Note 3: According to Lemma 1, the fuzzy logic systems can uniformly approximate a real continuous nonlinear function $f(x)$ on the compact set Ω . Hence, there exists an ideal parameter vector θ^* and the approximation error ε , which satisfy $f(x) = \theta^{*T} \zeta(x) + \varepsilon$ with $|\varepsilon| \leq \varepsilon^*, \forall x \in \Omega$, where ε^* is an unknown positive constant. It should be noted that the ideal parameter vector θ^* is only utilized for analytical purposes and that the estimate parameter vector $\hat{\theta}$ is utilized for control law design.

2.3. Preliminaries

Throughout this paper, the following assumptions and lemmas are used to analyze the main results.

Assumption 1. The uncertain nonlinear dynamic $\Delta_n(\bar{x}_n(t))$ in system (1) is bounded, and there exists $|\Delta_n(\bar{x}_n(t))| \leq \Delta_n^*$ with Δ_n^* being a positive constant.

Assumption 2. The desired reference trajectory y_d is bounded, and its first-, second-order derivatives exist and belong to compact set Ξ_1 . Then there exists a positive constant K_0 such that $\Xi_1 : \{(y_d, \dot{y}_d, \ddot{y}_d) : y_d^2 + \dot{y}_d^2 + \ddot{y}_d^2 \leq K_0\}$.

Lemma 2 [15]. For any $b \in R$ and $\vartheta > 0$, the hyperbolic tangent function $\tanh(\cdot)$ satisfies:

$$\begin{cases} 0 \leq |b| - b \tanh(\frac{b}{\vartheta}) \leq 0.2785\vartheta \\ 0 \leq b \tanh(\frac{b}{\vartheta}) \end{cases} \tag{8}$$

Lemma 3 [15]. For any variables $x \in R$ and $y \in R$, the following inequality holds:

$$xy \leq \frac{v^p}{p} |x|^p + \frac{1}{qv^q} |y|^q \tag{9}$$

where $v > 0, p > 1, q > 1$ and $(p - 1)(q - 1) = 1$.

Note 4: For Assumption 1, it is the stability condition of the controllability n order nonlinear system (1), which can ensure the design of the subsequent virtual control laws and the final control law. It should be noted that the boundedness of $\Delta_n(\bar{x}_n(t))$ is considered for the purpose of theoretical analysis. For Assumption 2, it is a common and fairly standard condition for the adaptive tracking control under the dynamic surface control design framework and can be seen in [8,9,13].

For the convenience of discussion in the next section, the time variable t will be ignored without causing confusion.

3. Adaptive Fuzzy Dynamic Surface Controller Design

In this section, the fuzzy logic systems are introduced to approximate the unknown smooth nonlinear function, and then an adaptive fuzzy control scheme with dynamic surface control technique is addressed. The control law design is based on the following change of coordinates:

$$\begin{cases} S_1 = e_1 = x_1 - y_d \\ S_i = x_i - y_{id}, i = 2, 3, \dots, n \end{cases} \tag{10}$$

where e_1 is the tracking error and y_{id} is the output of a given first-order filter with the virtual control law ψ_{id} as the input; S_1, S_2, \dots, S_n are the defined sliding mode switching functions.

The design procedure involves n steps. In step $i - 1 (i = 2, \dots, n)$, the virtual control law ψ_{id} is proposed to make the corresponding subsystem toward the equilibrium position, and in step n , the actual control law $u(t)$ will be developed.

Step 1. Considering the subsystem $\dot{x}_1 = x_2 + f_1(\bar{x}_1)$ and noting (10), the derivative of S_1 is obtained as:

$$\dot{S}_1 = x_2 + f_1(\bar{x}_1) - \dot{y}_d \tag{11}$$

According to Lemma 1, the first fuzzy logic system is utilized to approximate the unknown smooth nonlinear function $f_1(\bar{x}_1)$ as follows:

$$f_1(\bar{x}_1) = (\theta_1^*)^T \xi_1(\bar{x}_1) + \varepsilon_1(\bar{x}_1) \tag{12}$$

where $|\varepsilon_1(\bar{x}_1)| \leq \varepsilon_1^*$ with ε_1^* being a positive constant.

Choosing $V(S_1) = S_1^2/2$ and differentiating $V(S_1)$ along (11) gives:

$$\dot{V}(S_1) = S_1 x_2 + S_1 f_1(\bar{x}_1) - S_1 \dot{y}_d \tag{13}$$

Substituting (12) into (13) results in:

$$\dot{V}(S_1) \leq S_1 x_2 + S_1 (\theta_1^*)^T \xi_1(\bar{x}_1) + |S_1| \varepsilon_1^* - S_1 \dot{y}_d \tag{14}$$

By virtue of (14), the virtual control law ψ_{2d} and the adaptation law $\dot{\hat{\theta}}_1$ are hence designed as:

$$\psi_{2d} = -(\hat{\theta}_1)^T \xi_1(\bar{x}_1) - \varepsilon_1^* \tanh\left(\frac{\varepsilon_1^* S_1}{\vartheta}\right) - c_1 S_1 + \dot{y}_d \tag{15}$$

$$\dot{\hat{\theta}}_1 = \Phi_1 \xi_1(\bar{x}_1) S_1 - \eta_1 \Phi_1 (\hat{\theta}_1 - \hat{\theta}_1^0) \tag{16}$$

where $c_1 > 0$ and $\eta_1 > 0$ are the designed parameters; Φ_1 is the positive definite symmetric matrix to be designed; $\hat{\theta}_1$ is the estimate of ideal parameter vector θ_1^* of the first fuzzy logic system; and $\hat{\theta}_1^0$ is the initial parameter vector.

In order to avoid differentiating the virtual control law ψ_{2d} in the next step, the first-order filter with time constant τ_2 is introduced to filter the control law ψ_{2d} and then we have:

$$\tau_2 \dot{y}_{2d} + y_{2d} = \psi_{2d}, \psi_{2d}(0) = y_{2d}(0) \tag{17}$$

where y_{2d} is the output of the first-order filter, $\psi_{2d}(0)$ which is given an initial value.

Furthermore, defining the filter error of the first-order filter as $z_2 = y_{2d} - \psi_{2d}$, it is obtained from (17) that $\dot{y}_{2d} = -(z_2 / \tau_2)$. Thus, taking the derivative of z_2 gives:

$$\begin{aligned} \dot{z}_2 &= -\frac{z_2}{\tau_2} - \left(\frac{\partial \psi_{2d}}{\partial \hat{\theta}_1} \dot{\hat{\theta}}_1 + \frac{\partial \psi_{2d}}{\partial \bar{x}_1} \dot{\bar{x}}_1 + \frac{\partial \psi_{2d}}{\partial S_1} \dot{S}_1 - \frac{\partial \psi_{2d}}{\partial y_d} \dot{y}_d \right) \\ &= -\frac{z_2}{\tau_2} + H_2(S_1, S_2, z_2, \hat{\theta}_1, y_d, \dot{y}_d, \ddot{y}_d) \end{aligned} \tag{18}$$

where $H_2(\cdot)$ is the introduced nonnegative continuous function, and it is to be applied for the stability analysis in the next section.

Choosing $V(z_2) = z_2^2 / 2$, and using Lemma 3, differentiating $V(z_2)$ along (18) yields:

$$\dot{V}(z_2) \leq -\frac{z_2^2}{\tau_2} + |z_2| H_2 \leq -\left(\frac{1}{\tau_2} - \frac{1}{2}\right) z_2^2 + \frac{H_2^2}{2} \tag{19}$$

In addition, note that $x_2 = S_2 + y_{2d}$ and $z_2 = y_{2d} - \psi_{2d}$, and then:

$$x_2 = S_2 + z_2 + \psi_{2d} \tag{20}$$

According to Lemma 2, substituting (15) and (20) into (14) obtains:

$$\dot{V}(S_1) \leq -c_1 S_1^2 + S_1 S_2 + S_1 z_2 - S_1 (\tilde{\theta}_1)^T \xi_1(\bar{x}_1) + 0.2785\vartheta \tag{21}$$

where $\tilde{\theta}_1 = \hat{\theta}_1 - \theta_1^*$, $\tilde{\theta}_1$ represents the estimation error.

Designing the following Lyapunov function candidate:

$$V_1 = V(S_1) + V(z_2) + \frac{1}{2} (\tilde{\theta}_1)^T \Phi_1^{-1} \tilde{\theta}_1 \tag{22}$$

Taking the time derivative of V_1 and substituting (19) and (21), we obtain:

$$\dot{V}_1 \leq -c_1 S_1^2 + S_1 S_2 + S_1 z_2 - \left(\frac{1}{\tau_2} - \frac{1}{2}\right) z_2^2 - S_1 (\tilde{\theta}_1)^T \xi_1(\bar{x}_1) + (\tilde{\theta}_1)^T \Phi_1^{-1} \dot{\tilde{\theta}}_1 + \frac{H_2^2}{2} + 0.2785\vartheta \tag{23}$$

By virtue of $\dot{\tilde{\theta}}_1 = \dot{\hat{\theta}}_1$ and Lemma 3, we obtain:

$$(\tilde{\theta}_1)^T (\dot{\hat{\theta}}_1 - \dot{\theta}_1^0) = (\tilde{\theta}_1)^T (\dot{\tilde{\theta}}_1 + \dot{\theta}_1^* - \dot{\theta}_1^0) \geq \frac{1}{2} (\tilde{\theta}_1)^T (\dot{\tilde{\theta}}_1) - \frac{1}{2} (\theta_1^* - \hat{\theta}_1^0)^T (\theta_1^* - \hat{\theta}_1^0) \tag{24}$$

Then, substituting (16) and (24) into (23) becomes:

$$\dot{V}_1 \leq -c_1 S_1^2 - \left(\frac{1}{\tau_2} - \frac{1}{2}\right) z_2^2 - \frac{\eta_1}{2} (\tilde{\theta}_1)^T (\tilde{\theta}_1) + S_1 S_2 + S_1 z_2 + \frac{H_2^2}{2} + \frac{\eta_1}{2} (\theta_1^* - \hat{\theta}_1^0)^T (\theta_1^* - \hat{\theta}_1^0) + 0.2785\vartheta \tag{25}$$

Step i ($2 \leq i \leq n - 1$). Considering the subsystem $\dot{x}_i = x_{i+1} + f_i(\bar{x}_i)$ and noting (10), the derivative of S_i is obtained as:

$$\dot{S}_i = x_i + f_i(\bar{x}_i) - \dot{y}_{id} \tag{26}$$

The i th fuzzy logic system is used to approximate the unknown smooth nonlinear function $f_i(\bar{x}_i)$ as follows:

$$f_i(\bar{x}_i) = (\theta_i^*)^T \zeta_i(\bar{x}_i) + \varepsilon_i(\bar{x}_i) \tag{27}$$

where $|\varepsilon_i(\bar{x}_i)| \leq \varepsilon_i^*$ with ε_i^* as a positive constant.

Similarly, considering $V(S_i) = S_i^2/2$ and differentiating $V(S_i)$ along (26) gives:

$$\dot{V}(S_i) \leq S_i x_{i+1} + S_i \left((\theta_i^*)^T \zeta_i(\bar{x}_i) - \dot{y}_{id} \right) + |S_i| \varepsilon_i^* \tag{28}$$

Designing the virtual control law $\psi_{(i+1)d}$ and the adaptation law $\hat{\theta}_i$ as follows:

$$\psi_{(i+1)d} = -(\hat{\theta}_i)^T \zeta_i(\bar{x}_i) - \varepsilon_i^* \tanh\left(\frac{\varepsilon_i^* S_i}{\vartheta}\right) - c_i S_i - S_{i-1} + \dot{y}_{id} \tag{29}$$

$$\dot{\hat{\theta}}_i = \Phi_i \zeta_i(\bar{x}_i) S_i - \eta_i \Phi_i (\hat{\theta}_i - \hat{\theta}_i^0) \tag{30}$$

where $c_i > 0$ and $\eta_i > 0$ are the designed parameters, Φ_i is the positive definite symmetric matrix to be designed, $\hat{\theta}_i$ is the estimate of the ideal parameter vector θ_i^* of the i th fuzzy logic system, and $\hat{\theta}_i^0$ is the initial parameter vector.

Let $\psi_{(i+1)d}$ pass through the first-order filter with time constant τ_{i+1} , and then we obtain $y_{(i+1)d}$ as:

$$\tau_{i+1} \dot{y}_{(i+1)d} + y_{(i+1)d} = \psi_{(i+1)d}, \psi_{(i+1)d}(0) = y_{(i+1)d}(0) \tag{31}$$

where $y_{(i+1)d}$ is the output of first-order filter, $\psi_{(i+1)d}(0)$ is given an initial value.

Defining the filter error of the first-order filter as $z_{i+1} = y_{(i+1)d} - \psi_{(i+1)d}$ and considering $\dot{y}_{(i+1)d} = -(z_{i+1}/\tau_{i+1})$, we obtain:

$$\begin{aligned} \dot{z}_{i+1} &= -\frac{z_{i+1}}{\tau_{i+1}} - \left(\frac{\partial \psi_{(i+1)d}}{\partial \hat{\theta}_i} \dot{\hat{\theta}}_i + \frac{\partial \psi_{(i+1)d}}{\partial \bar{x}_i} \dot{\bar{x}}_i + \frac{\partial \psi_{(i+1)d}}{\partial S_i} \dot{S}_i - \frac{\partial \psi_{(i+1)d}}{\partial \dot{y}_{(i+1)d}} \ddot{y}_{(i+1)d} \right) \\ &= -\frac{z_{i+1}}{\tau_{i+1}} + H_{i+1}(S_1, S_2, \dots, S_{i+1}, z_2, z_3, \dots, z_{i+1}, \hat{\theta}_1, \hat{\theta}_2, \dots, \hat{\theta}_i, y_d, \dot{y}_d, \ddot{y}_d) \end{aligned} \tag{32}$$

where $H_{i+1}(\cdot)$ is the introduced nonnegative continuous function.

Correspondingly, choosing $V(z_{i+1}) = z_{i+1}^2/2$ and using Lemma 3, differentiating $V(z_{i+1})$ along (32) yields:

$$\dot{V}(z_{i+1}) \leq -\left(\frac{1}{\tau_{i+1}} - \frac{1}{2}\right) z_{i+1}^2 + \frac{H_{i+1}^2}{2} \tag{33}$$

Furthermore, considering $x_{i+1} = S_{i+1} + z_{i+1} + \psi_{(i+1)d}$ and (29), (28) can be rewritten as:

$$\dot{V}(S_i) \leq -c_i S_i^2 - S_{i-1} S_i + S_i S_{i+1} + S_i z_{i+1} - S_i (\tilde{\theta}_i)^T \zeta_i(\bar{x}_i) + 0.2785\vartheta \tag{34}$$

Designing the Lyapunov function V_i as follows:

$$V_i = V(S_i) + V(Z_{i+1}) + \frac{1}{2}(\tilde{\theta}_i)^T \Phi_1^{-1} \tilde{\theta}_i \tag{35}$$

where $\tilde{\theta}_i = \hat{\theta}_i - \theta_i^*$, and $\tilde{\theta}_i$ represents the estimation error.

Thus, according to (30), (33), (34), and Lemma 3, we obtain:

$$\begin{aligned} \dot{V}_i \leq & -c_i S_i^2 - \left(\frac{1}{\tau_{i+1}} - \frac{1}{2}\right) z_{i+1}^2 - \frac{\eta_i}{2} (\tilde{\theta}_i)^T (\tilde{\theta}_i) - S_{i-1} S_i + S_i S_{i+1} + S_i z_{i+1} + \frac{H_{i+1}^2}{2} + 0.2785\vartheta \\ & + \frac{\eta_i}{2} (\theta_i^* - \hat{\theta}_i^0)^T (\theta_i^* - \hat{\theta}_i^0) \end{aligned} \tag{36}$$

Step n. This is the last step. Considering the subsystem $\dot{x}_n(t) = v(t) + f_n(\bar{x}_n) + \Delta_n(\bar{x}_n)$ and noting (2) and (10), we obtain:

$$\dot{S}_n = \rho u(t) + f_0(t) + f_n(\bar{x}_n) + \Delta_n(\bar{x}_n) - \dot{y}_{nd} \tag{37}$$

Considering the n th fuzzy logic system, then we obtain:

$$f_n(\bar{x}_n) = (\theta_n^*)^T \xi_n(\bar{x}_n) + \varepsilon_n(\bar{x}_n) \tag{38}$$

where $|\varepsilon_n(\bar{x}_n)| \leq \varepsilon_n^*$ with ε_n^* as a positive constant.

Similarly, choosing $V(S_n) = S_n^2/2$, and considering (37) and (38), it is obtained that:

$$\dot{V}(S_n) \leq S_n \left(\rho u(t) + (\theta_n^*)^T \xi_n(\bar{x}_n) - \dot{y}_{nd} \right) + |S_n| \mu_n^* \tag{39}$$

where $\mu_n^* = f_0^* + \varepsilon_n^* + \Delta_n^*$.

Taking,

$$\alpha_n(t) = (\hat{\theta}_n)^T \xi_n(\bar{x}_n) + \mu_n^* \tanh\left(\frac{\mu_n^* S_n}{\vartheta}\right) + c_n S_n + S_{n-1} - \dot{y}_{nd} \tag{40}$$

where $c_n > 0$ is the designed parameter.

Due to ρ being an unknown constant, let $\delta_n = 1/\rho$ and $\hat{\delta}_n$ be the estimate of δ_n , then the following control law $u(t)$ and adaptation laws $\hat{\theta}_n$ and $\hat{\delta}_n$ are designed as:

$$u(t) = -\hat{\delta}_n \alpha_n(t) \tag{41}$$

$$\dot{\hat{\theta}}_n = \Phi_n \xi_n(\bar{x}_n) S_n - \eta_n \Phi_n (\hat{\theta}_n - \hat{\theta}_n^0) \tag{42}$$

$$\dot{\hat{\delta}}_n = S_n \alpha_n(t) - \pi_n \hat{\delta}_n \tag{43}$$

where $\eta_n > 0$ and $\pi_n > 0$ are the designed parameters; Φ_n is the positive definite symmetric matrix to be designed; $\hat{\theta}_n$ is the estimate of ideal parameter vector θ_n^* of the n th fuzzy logic system and $\hat{\theta}_n^0$ is the initial parameter vector.

Choosing the Lyapunov function V_n as:

$$V_n = V(S_n) + \frac{1}{2}(\tilde{\theta}_n)^T \Phi_n^{-1} \tilde{\theta}_n \tag{44}$$

where $\tilde{\theta}_n = \hat{\theta}_n - \theta_n^*$, and $\tilde{\theta}_n$ represents the estimation error.

Similarly, following the same way of step i and considering (41) and (42), we obtain:

$$\dot{V}_n \leq S_n (\alpha_n - \rho \hat{\delta}_n \alpha_n) - c_n S_n^2 - \frac{\eta_n}{2} (\tilde{\theta}_n)^T (\tilde{\theta}_n) - S_{n-1} S_n + \frac{\eta_n}{2} (\theta_n^* - \hat{\theta}_n^0)^T (\theta_n^* - \hat{\theta}_n^0) + 0.2785\vartheta \tag{45}$$

So far, the design process of the adaptive fuzzy dynamic surface controller has been completed.

Note 5: In this paper, the adaptive fuzzy dynamic surface control law is applied for the uncertain nonlinear systems with actuator faults. Based on the application of dynamic surface control technology, the derivation of nonlinear terms in the design of virtual control laws and the final actual control law is avoided. In addition, we also found that in some studies, such as references [20–22], the command filter control method is introduced to improve the traditional backstepping control method. It is found that the implementation of the command filter control method needs to introduce a compensation signal and then construct the compensation signal error. Hence, by comparison, the implementation of the dynamic surface control method is more intuitive and only needs to design a kind of first-order low-pass filter. Then, the design of the virtual control law and final actual control law can be well simplified. However, the command filter also has its own advantages, which can still well avoid the explosion of complexity problems in the design of virtual control laws and adaptive updating laws.

4. Stability Analysis

In this section, the stability analysis is elaborated and it is proved that all of the signals in the closed-loop system are semi-global bounded.

Theorem 1. *Considering the uncertain nonlinear system with actuator fault (1) under the Assumptions 1 and 2, the virtual control laws are designed as (15) and (29) with the adaptation laws constructed as (16) and (30), and the control law is designed as (41) with (40) and the adaptation laws constructed as (42) and (43), then there exist $c_i, \eta_i, \Phi_i (i = 1, 2, \dots, n), \tau_i (i = 2, \dots, n), \pi_n$ and ϑ such that all of the signals in the closed-loop system are semi-global bounded and the tracking error can be guaranteed to converge to the specified small neighborhood of the origin by adjusting the control law parameters.*

Proof: Consider the Lyapunov function as follows:

$$V = \sum_{i=1}^n V_i + \frac{\rho}{2} \tilde{\delta}_n^2 \tag{46}$$

where $\tilde{\delta}_n = \hat{\delta}_n - \delta_n$, and $\tilde{\delta}_n$ represents the estimation error.

It follows from (25), (36), and (45) that the time derivative of V yields:

$$\begin{aligned} \dot{V} \leq & S_n(\alpha_n - \rho \hat{\delta}_n \alpha_n) - \sum_{i=1}^n c_i S_i^2 - \sum_{i=2}^n \left(\frac{1}{\tau_i} - \frac{1}{2}\right) z_i^2 - \sum_{i=1}^n \frac{\eta_i}{2} (\tilde{\theta}_i)^T (\tilde{\theta}_i) + \sum_{i=1}^{n-1} S_i z_{i+1} + \rho \tilde{\delta}_n \dot{\tilde{\delta}}_n \\ & + \sum_{i=1}^n \frac{\eta_i (\theta_i^* - \hat{\theta}_i^0)^T (\theta_i^* - \hat{\theta}_i^0)}{2} + \sum_{i=1}^n \frac{H_i^2}{2} + 0.2785n\vartheta \end{aligned} \tag{47}$$

Based on Lemma 3, we obtain:

$$S_i z_{i+1} \leq \frac{S_i^2}{2} + \frac{z_{i+1}^2}{2} \tag{48}$$

$$\tilde{\delta}_n \hat{\delta}_n = \tilde{\delta}_n (\tilde{\delta}_n + \delta_n) \geq \frac{1}{2} \tilde{\delta}_n^2 - \frac{1}{2} \delta_n^2 \tag{49}$$

Substituting (43), (48), and (49) into (47), and letting $\lambda_{\max}(\Phi_i^{-1})$ be the maximum eigenvalue of Φ_i^{-1} , then we obtain:

$$\begin{aligned} \dot{V} \leq & - \sum_{i=1}^{n-1} \left(c_i - \frac{1}{2}\right) S_i^2 - c_n S_n^2 - \sum_{i=2}^n \left(\frac{1}{\tau_i} - 1\right) z_i^2 - \sum_{i=1}^n \frac{\eta_i}{2\lambda_{\max}(\Phi_i^{-1})} (\tilde{\theta}_i)^T \Phi_i^{-1} (\tilde{\theta}_i) - \frac{\pi_n \rho}{2} \tilde{\delta}_n^2 \\ & + \sum_{i=1}^n \frac{\eta_i (\theta_i^* - \hat{\theta}_i^0)^T (\theta_i^* - \hat{\theta}_i^0)}{2} + \sum_{i=2}^n \frac{H_i^2}{2} + \frac{\pi_n \rho}{2} \delta_n^2 + 0.2785n\vartheta \end{aligned} \tag{50}$$

Taking,

$$c_i \geq \frac{1}{2} + \phi, i = 1, 2, \dots, n - 1 \tag{51}$$

$$c_n \geq \phi \tag{52}$$

$$\frac{1}{\tau_i} \geq 1 + \phi, i = 2, 3, \dots, n \tag{53}$$

$$\eta_i \geq 2\phi\lambda_{\max}(\Phi_i^{-1}), i = 1, 2, \dots, n \tag{54}$$

$$\pi_n \geq 2\phi \tag{55}$$

where ϕ is a designed constant.

Define the following compact set as:

$$\Xi_i = \left\{ (S_1, \dots, S_i, z_2, \dots, z_i, \tilde{\theta}_1, \dots, \tilde{\theta}_i, \tilde{\delta}_n) : S_1^2 + (\tilde{\theta}_1)^T \Phi_1^{-1} \tilde{\theta}_1 + \tilde{\delta}_n^2 + \sum_{j=2}^i (S_j^2 + z_j^2 + (\tilde{\theta}_j)^T \Phi_j^{-1} \tilde{\theta}_j) \leq 2\chi \right\} \tag{56}$$

where $i = 2, \dots, n$.

Noting the Assumption 2, the set Ξ_1 is compact, and then it is clear to find from (32) that all of the variables of nonnegative continuous function $H_i(\cdot)$ are in the compact set $\Xi_1 \times \Xi_i$. Therefore, the function $|H_i(\cdot)|$ has a maximum in the compact set $\Xi_1 \times \Xi_i$. Without loss of generality, let the maximum of $|H_i(\cdot)|$ be H_{iM} .

From (51)–(55), obviously, we can obtain:

$$\dot{V} \leq -2\phi \left(\frac{1}{2} \sum_{i=1}^n S_i^2 + \frac{1}{2} \sum_{i=2}^n z_i^2 + \frac{1}{2} \sum_{i=1}^n (\tilde{\theta}_i)^T \Phi_i^{-1} (\tilde{\theta}_i) + \frac{1}{2} \rho \tilde{\delta}_n^2 \right) + P_0 = -2\phi V + P_0 \tag{57}$$

where $P_0 = \sum_{i=1}^n \frac{\eta_i(\theta_i^* - \hat{\theta}_i^0)^T (\theta_i^* - \hat{\theta}_i^0)}{2} + \sum_{i=2}^n \frac{H_{iM}^2}{2} + \frac{\pi_n \rho}{2} \delta_n^2 + 0.2785n\vartheta$.

Which further implies that:

$$V(t) \leq (V(0) - P_1)e^{-2\phi t} + P_1 \leq V(0) + P_1 \tag{58}$$

where $P_1 = P_0 / (2\phi)$.

From (57), this signifies that $S_i, z_i, \tilde{\theta}_i$ and $\tilde{\delta}_n$ are bounded, and $\hat{\theta}_i = \tilde{\theta}_i + \theta_i^*$ is bounded due to the boundedness of $\tilde{\theta}_i$ and θ_i^* . Since $e_1 = S_1 = x_1 - y_d$ and y_d are both bounded, then x_1 is bounded. Considering ψ_{2d} is a function on the bounded signals $S_1, \hat{\theta}_1, y_d$, and \dot{y}_d , then we can obtain ψ_{2d} is also bounded. Because of $x_2 = S_2 + z_2 + \psi_{2d}$, then there exists x_2 , which is bounded. Similarly, we can obtain that ψ_{id} and x_i with $i = 3, 4, \dots, n$ are bounded. Consequently, it can be proved that all of the signals of the closed-loop system are bounded.

Moreover, considering $V(S_i) = S_i^2 / 2$ and (46), we obtain:

$$\sum_{i=1}^n \frac{S_i^2}{2} \leq V(t) \tag{59}$$

and the following inequality from (58) holds:

$$\lim_{t \rightarrow \infty} |e_1| \leq \sqrt{2P_1} \tag{60}$$

Noting $P_1 = P_0 / (2\phi)$ lies on the designed parameters $c_i, \eta_i, \Phi_i, \tau_i, \pi_n$ and ϑ , which means that the tracking error e_1 can be guaranteed to converge to the specified small neighborhood of the origin by properly adjusting these designed parameters. This completes the proof. \square

Note 6. There are numerous parameters to be designed in this paper, but several parameters are introduced only for the theoretical analysis, e.g., ρ_0 and θ^* . Moreover, several parameters such as $f_0^*, \varepsilon_1^*, \varepsilon_i^*, \varepsilon_n^*$ and Δ_n^* , only require an appropriate upper bound without influencing the control performance. The main design parameters in this paper include $c_i, \eta_i, \Phi_i, \tau_i, \pi_n$ and ϑ . From $\lim_{t \rightarrow \infty} |e_1| \leq \sqrt{2P_1}$, where $P_1 = P_0/(2\varphi)$, the tracking error e_1 can be made smaller by increasing η_i, τ_i, π_n , and ϑ or decreasing Φ_i and c_i .

5. Simulation Analysis

In this section, the effectiveness of the designed control approach described in Section 3 will be illustrated by two cases.

Case 1. Consider the following third-order uncertain nonlinear system [43]:

$$\begin{cases} \dot{x}_1 = x_2 + 2x_1^2 \sin(x_1) \\ \dot{x}_2 = x_3 + x_1^2 + x_1x_2 + x_2 \cos(x_1) \\ \dot{x}_3 = v(t) + x_1x_3 + x_2^2 + x_3 \sin(x_2) + \Delta_3(\bar{x}_3(t)) \\ y = x_1 \end{cases} \tag{61}$$

where $\Delta_3(\bar{x}_3(t))$ is the uncertain dynamic which is given as $\Delta_3(\bar{x}_3(t)) = 0.1 \sin(t)$. Compared with (1), we obtain:

$$\begin{cases} f_1(\bar{x}_1(t)) = 2x_1^2 \sin(x_1) \\ f_2(\bar{x}_2(t)) = x_1^2 + x_1x_2 + x_2 \cos(x_1) \\ f_3(\bar{x}_3(t)) = x_1x_3 + x_2^2 + x_3 \sin(x_2) \end{cases} \tag{62}$$

In this paper, it is assumed that the system (61) suffers from the actuator fault, for which the model of actuator faults is as shown in (2). In simulation analysis, let $\rho = 0.5 + 0.45 \sin(t), f_0(t) = 0.01 \sin(t)$ that occurs at $t = 5$ s, respectively.

The control purpose is to design a control law $u(t)$ such that the output of the closed-loop system (61) can approximate the reference signal $y_d = \sin(t)$ asymptotically. Based on the approach of this paper, the intermediate control signals and control laws are shown in Table 1.

Table 1. Intermediate control signals and control laws.

Error	Control Law	First-Order Filter and Adaptation Law
$e_1 = x_1 - y_d$ $S_1 = e_1$	$\psi_{2d} = -(\hat{\theta}_1)^T \xi_1(\bar{x}_1) - \varepsilon_1^* \tanh(\frac{\varepsilon_1^* S_1}{\vartheta})$ $-c_1 S_1 + \dot{y}_d$	$\tau_2 \dot{\psi}_{2d} + \psi_{2d} = \psi_{2d}, \psi_{2d}(0) = y_{2d}(0)$ $\hat{\theta}_1 = \Phi_1 \xi_1(\bar{x}_1) S_1 - \eta_1 \Phi_1 (\hat{\theta}_1 - \hat{\theta}_1^0)$
$z_2 = y_{2d} - \psi_{2d}$ $S_2 = x_2 - y_{2d}$	$\psi_{3d} = -(\hat{\theta}_2)^T \xi_2(\bar{x}_2) - \varepsilon_2^* \tanh(\frac{\varepsilon_2^* S_2}{\vartheta})$ $-c_2 S_2 - S_1 + \dot{y}_{2d}$	$\tau_3 \dot{\psi}_{3d} + \psi_{3d} = \psi_{3d}, \psi_{3d}(0) = y_{3d}(0)$ $\hat{\theta}_2 = \Phi_2 \xi_2(\bar{x}_2) S_2 - \eta_2 \Phi_2 (\hat{\theta}_2 - \hat{\theta}_2^0)$
$z_3 = y_{3d} - \psi_{3d}$ $S_3 = x_3 - y_{3d}$	$\alpha_3(t) = (\hat{\theta}_3)^T \xi_3(\bar{x}_3) + \mu_3^* \tanh(\frac{\mu_3^* S_3}{\vartheta})$ $+c_3 S_3 + S_2 - y_{3d}$ $u(t) = -\hat{\delta}_3 \alpha_3(t)$	$\dot{\delta}_3 = S_3 \alpha_3(t) - \pi_3 \delta_3$ $\hat{\theta}_3 = \Phi_3 \xi_3(\bar{x}_3) S_3 - \eta_3 \Phi_3 (\hat{\theta}_3 - \hat{\theta}_3^0)$

In the simulation analysis, the fuzzy sets are given as $F_1^1 = (NM), F_1^2 = (NS), F_1^3 = (ZO), F_1^4 = (PS), F_1^5 = (PM), F_2^1 = (NM), F_2^2 = (NS), F_2^3 = (ZO), F_2^4 = (PS), F_2^5 = (PM), F_3^1 = (NM), F_3^2 = (NS), F_3^3 = (ZO), F_3^4 = (PS)$ and $F_3^5 = (PM)$, which are specified in the interval $[-4, 4]$ for variables x_1, x_2 and x_3 , respectively. In addition, *NM, NS, ZO, PS, and PM* represent negative middle, negative small, zero, positive small, and positive middle with the center points being pointed as $-4, -2, 0, 2,$ and 4 , respectively. Accordingly, the fuzzy membership functions are denoted as $\mu_{NM} = \exp(-[(x_i - 4)/1.5]^2), \mu_{NS} = \exp(-[(x_i - 2)/1.5]^2), \mu_{ZO} = \exp(-[(x_i)/1.5]^2), \mu_{PS} = \exp(-[(x_i + 2)/1.5]^2)$ and $\mu_{PM} = \exp(-[(x_i + 4)/1.5]^2), i = 1, 2, 3$, respectively. The curves of fuzzy membership functions are shown in Figure 1. Take design parameters and initial conditions as: $\vartheta = 0.09, c_1 = 2.7, c_2 = 1.5, c_3 = 1.0, \varepsilon_1^* = 1.2, \varepsilon_2^* = 5.5, \mu_3^* = 4, \eta_1 = \eta_2 = \eta_3 = 10^{-3}, \Phi_1 = \text{diag}\{85\}, \Phi_2 = \text{diag}\{1\}, \Phi_3 = \text{diag}\{40\}$,

$$\tau_2 = \tau_3 = 0.02, \pi_3 = 5.0, [x_1(0), x_2(0), x_3(0)]^T = [1.0, 0.5, 0]^T, y_{2d}(0) = y_{3d}(0) = 0, \hat{\theta}_1^0(0) = \hat{\theta}_2^0(0) = \hat{\theta}_3^0(0) = 0.025, \hat{\delta}_3^0(0) = 0.01.$$

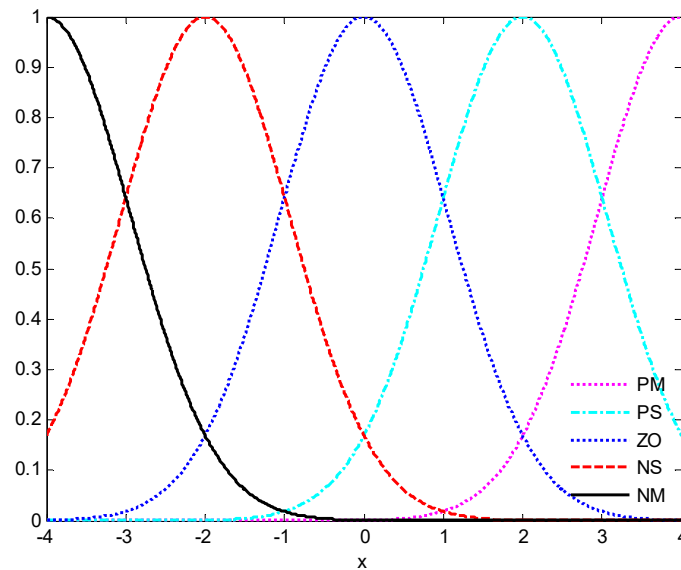


Figure 1. Fuzzy membership functions.

The simulation results of Case 1 are shown in Figures 2–9. It is found from Figures 2 and 3 that the excellent tracking performance can be achieved after a short transit process. Furthermore, the curves of nonlinear functions f_1, f_2, f_3 and their estimates $\hat{f}_1, \hat{f}_2, \hat{f}_3$ are shown in Figures 4–6, respectively. Figure 7 gives the curves of δ_3 and its estimate $\hat{\delta}_3$, and the control input $u(t)$ is displayed in Figure 8. Because of the initial values are randomly selected, the amplitude of the estimated value of functions f_2, f_3 , and δ_3 are greatly reduced compared with the actual value, which also shows that the control laws designed in this paper are effective from another point of view.

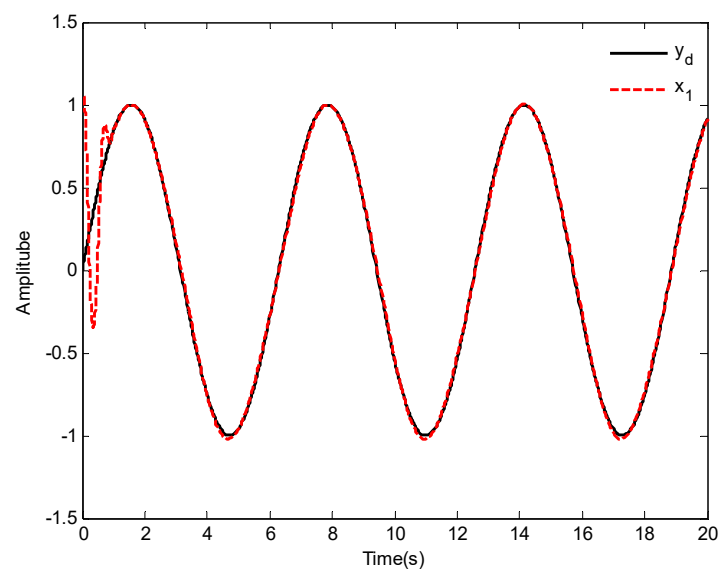


Figure 2. The curves of tracking performance.

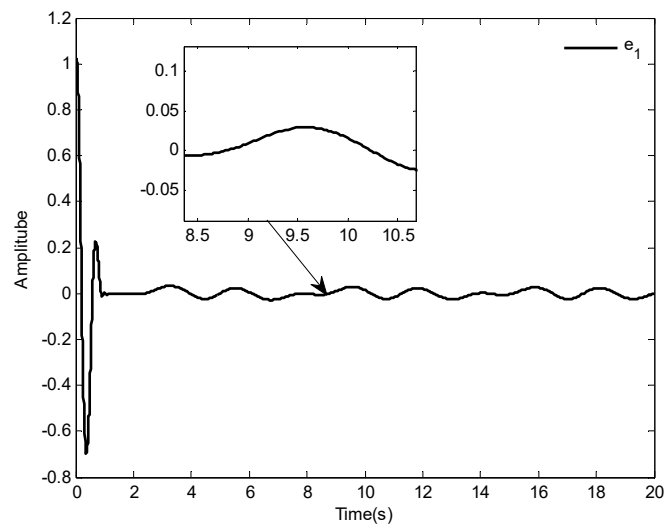


Figure 3. The curve of tracking error.

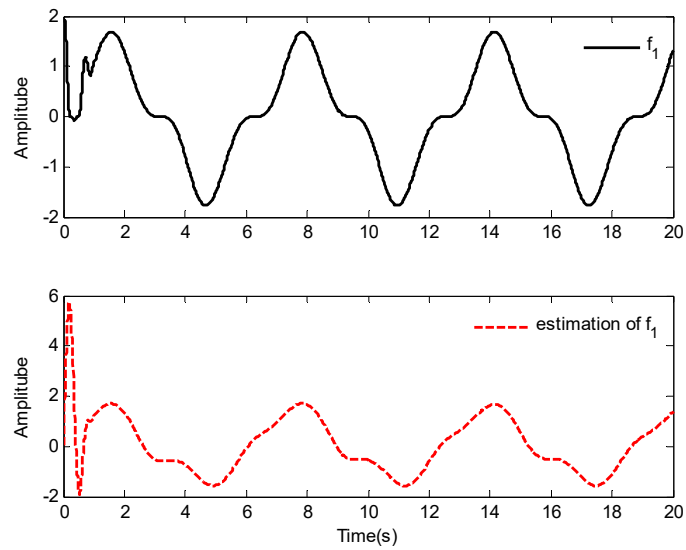


Figure 4. Response of f_1 and \hat{f}_1 .

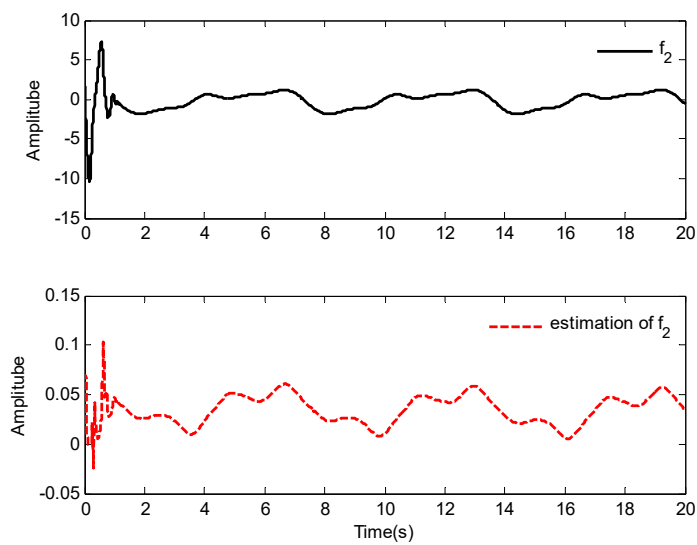


Figure 5. Response of f_2 and \hat{f}_2 .

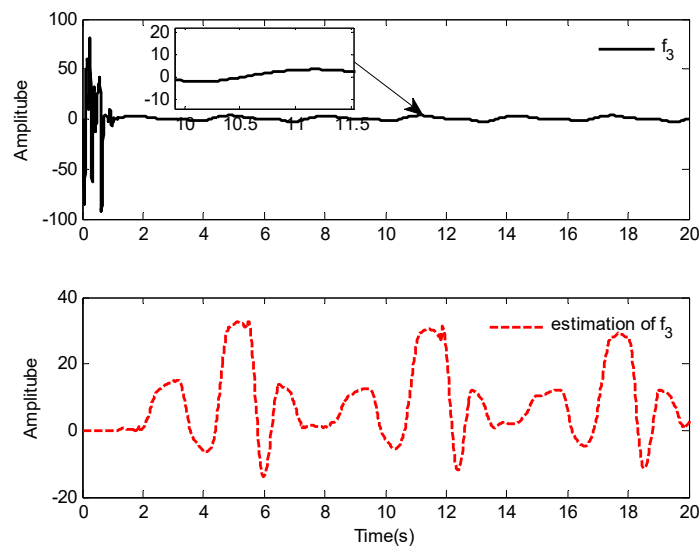


Figure 6. Response of f_3 and \hat{f}_3 .

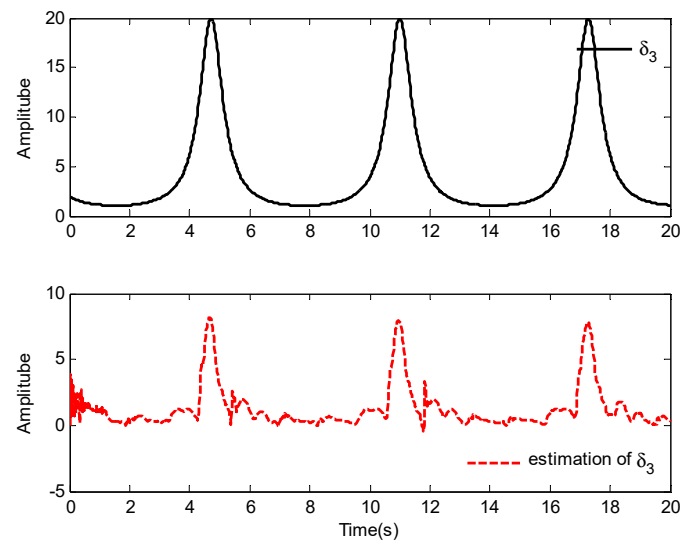


Figure 7. Response of δ_3 and $\hat{\delta}_3$.

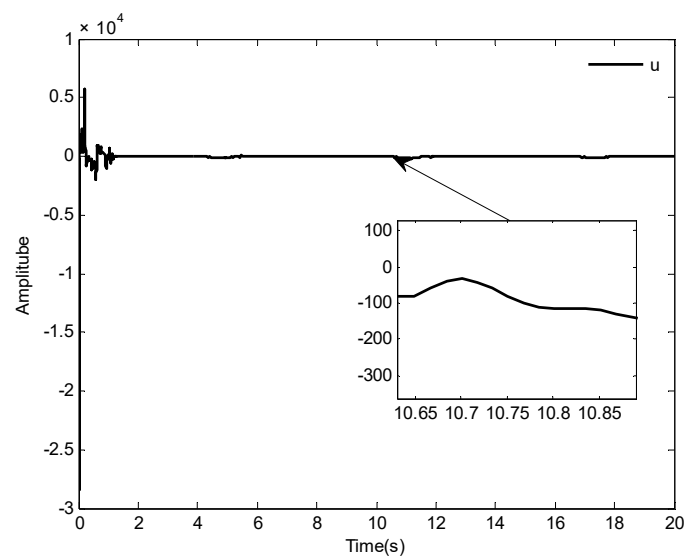


Figure 8. The curve of control input $u(t)$.

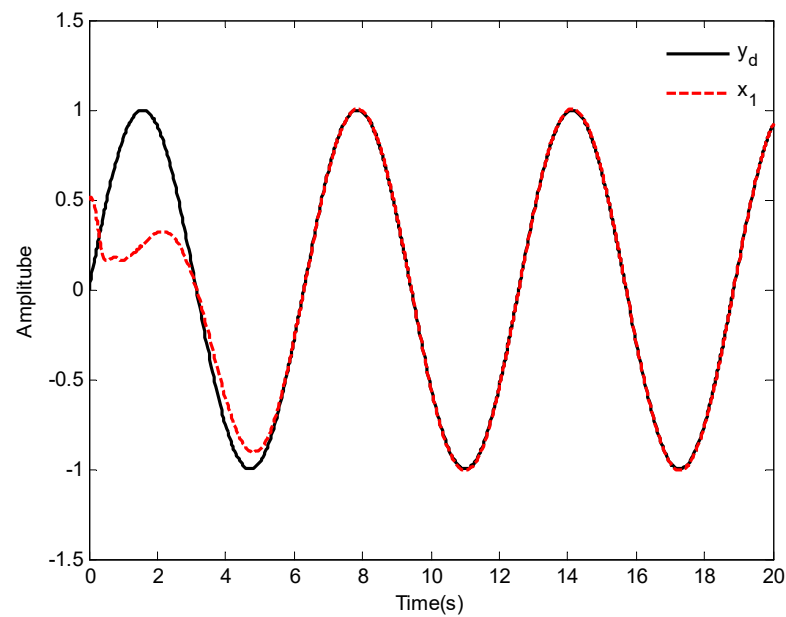


Figure 9. The curves of tracking performance.

Case 2. Consider a one-link manipulator actuated by a brush dc [9], the dynamic of the system is described as:

$$\begin{cases} C\ddot{p} + A\dot{p} + L \sin(p) = I + d_I \\ Q\dot{I} = -RI - K_m\dot{p} + U \end{cases} \quad (63)$$

where p , \dot{p} and \ddot{p} are the link angular position, velocity and acceleration, respectively. I is the motor current, d_I is the stochastic disturbance. U is the input voltage. The parameters of system (62) are given as $C = A = Q = 1$, $R = 0.5$, $L = 2.2$, and $K_m = 5$.

Let $x_1 = p$, $x_2 = \dot{p}$, $x_3 = \ddot{p}$ and $v(t) = U$, so system (63) can be rewritten as follows:

$$\begin{cases} \dot{x}_1 = x_2 \\ \dot{x}_2 = x_3 - 2.2 \sin(x_1) - x_2 + 4 \sin(t) \\ \dot{x}_3 = v(t) - 5x_2 - 0.5x_3 \\ y = x_1 \end{cases} \quad (64)$$

Compared with system (1), we have $f_1 = 0$, $f_2 = -2.2 \sin(x_1) - x_2 + 4 \sin(t)$, $f_3 = -5x_2 - 0.5x_3$ and $\Delta_3(\bar{x}_3(t)) = 0$. Due to the nonlinear function $f_1 = 0$, the adaptation law $\hat{\theta}_1$ will not appear in the control design. The actuator fault model is considered as (2).

The initial conditions are given as $[x_1(0), x_2(0), x_3(0)]^T = [0.5, 0.5, 0.5]^T$, the reference signal is given as $y_d = \sin(t)(1 - e^{-0.1t^2})$. Some simulation parameters are set as: $\vartheta = 0.15$, $\eta_2 = \eta_3 = 0.05$, $\tau_2 = 0.01$, $\tau_3 = 0.15$. Other parameters are the same as in Case 1. The simulation results are depicted in Figures 9–14.

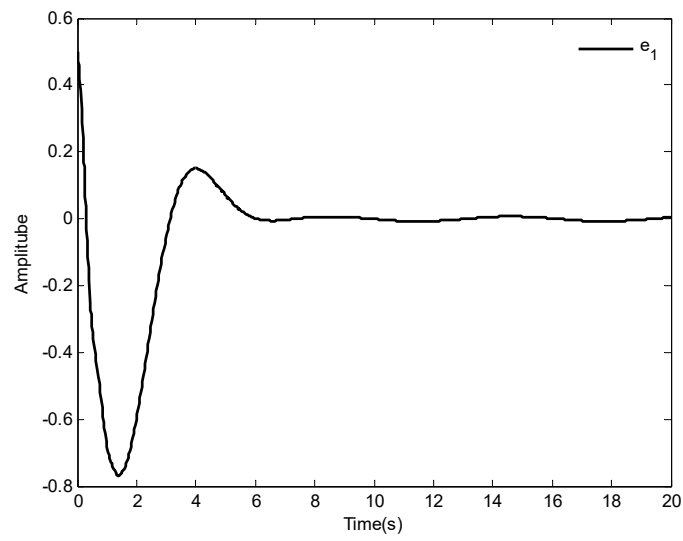


Figure 10. The curve of tacking error.

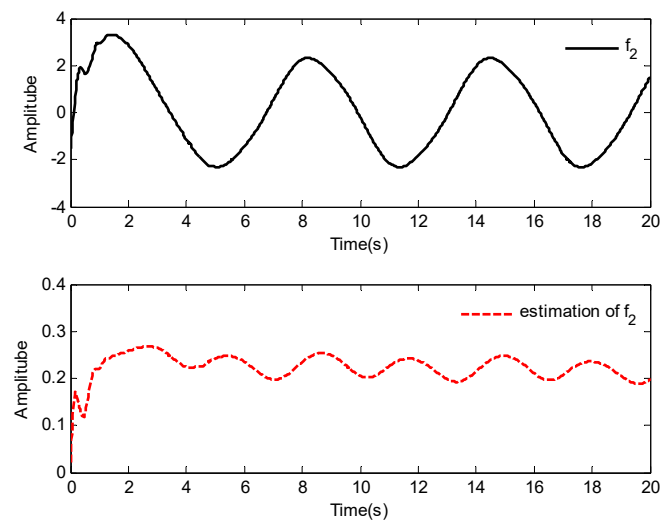


Figure 11. Response of f_2 and \hat{f}_2 .

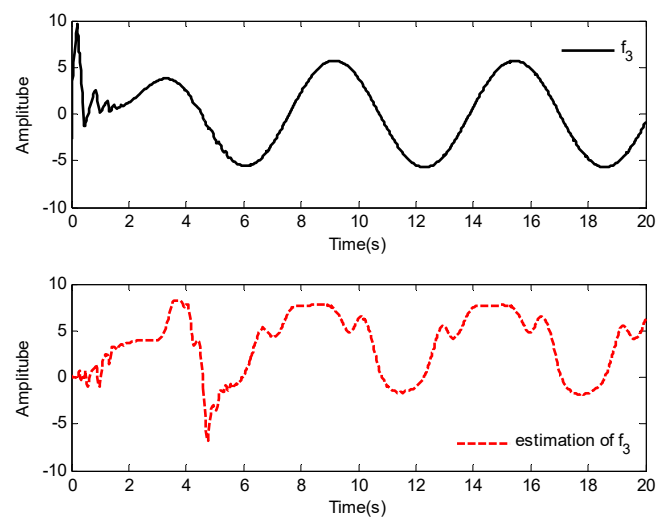


Figure 12. Response of f_3 and \hat{f}_3 .

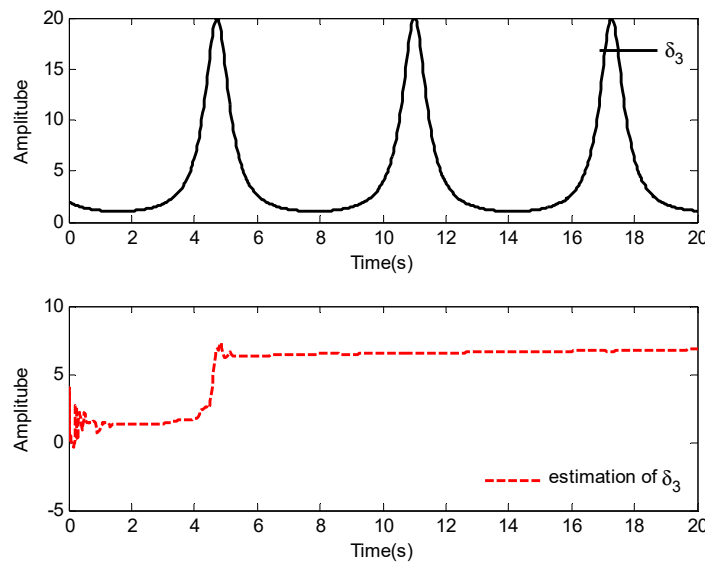


Figure 13. Response of δ_3 and $\hat{\delta}_3$.

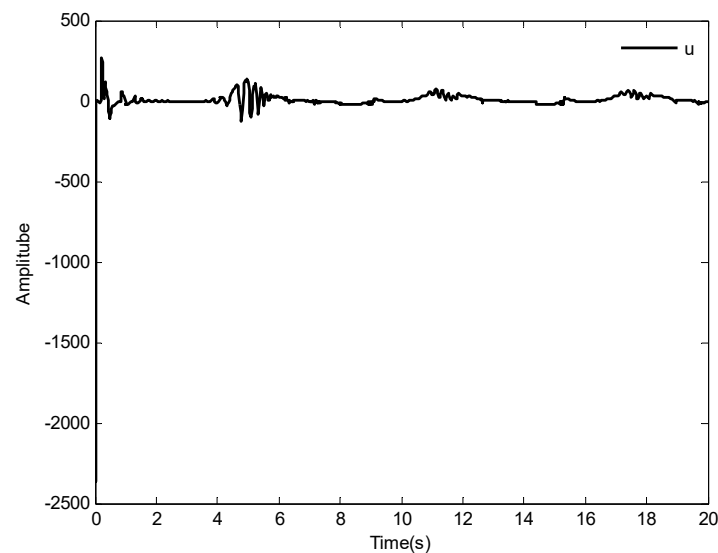


Figure 14. The curve of control input $u(t)$.

The tracking results and tracking error are shown in Figures 9 and 10, respectively. It is obviously found that the one-link manipulator actuated by a brush dc can obtain good tracking performance based on the application of the adaptive fuzzy dynamic surface control scheme proposed in this paper. Additionally, the nonlinear functions f_2, f_3 and their estimates \hat{f}_2, \hat{f}_3 are shown in Figures 11 and 12, respectively, and the curves of δ_3 and its estimate $\hat{\delta}_3$ is shown in Figure 13. The control input $u(t)$ is displayed in Figure 14. Similar to Case 1, due to the initial values being randomly selected, it can be found that the amplitude of the estimated value of functions f_2, f_3 , and δ_3 are greatly reduced compared with the actual value, which also implies that the control laws designed in this paper are effective from another point of view. Moreover, although the system considered is different, fairly good control performance can still be obtained by using the designed control laws.

Case 3. To further illustrate the effectiveness of the designed control law in practical system application, the system in [44] is considered. According to the description of [44], the model of ship can be rewritten as:

$$\begin{cases} \dot{x}_1 = x_2 \\ \dot{x}_2 = K_{ns}\omega_n^2 u_s(t) - 2\xi\omega_n x_2 - \omega_n^2 x_1 \end{cases} \quad (65)$$

where $x_1 = \Psi(t)$, $x_2 = \dot{\Psi}(t)$, $u_s(t) = o(t)$, $K_{ns} = 9.5 \times 10^{-7}$, $\omega_n = 1.25$ and $\zeta = 0.8$.

In addition, the initial states of system (64) are given as $x_1(0) = 35$ and $x_2(0) = 0$, the desired reference signal is given as $y_d = 10 \sin(t)$, the simulation $t = 30$ s, and the other models are the same as [44]. Based the proposed control law of this paper, the simulation results are shown in Figures 15–17.

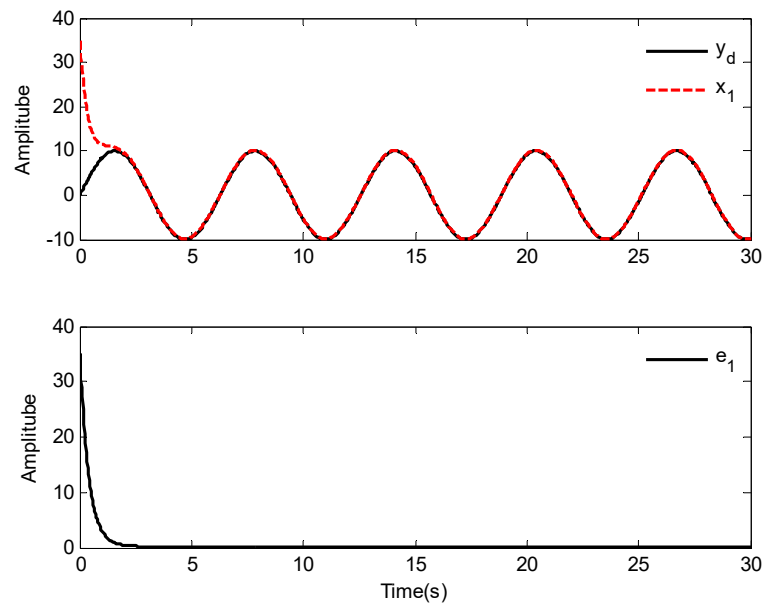


Figure 15. The curves of tracking performance and error.

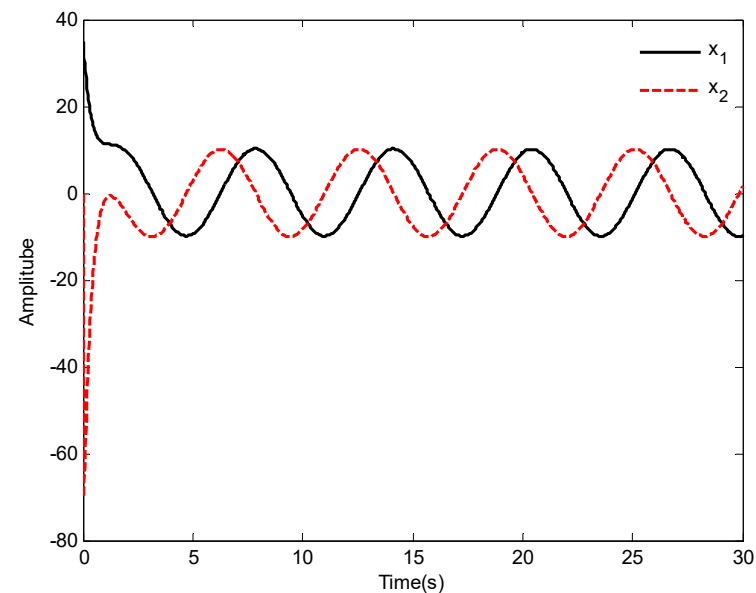


Figure 16. The curves of states x_1 and x_2 .

The tracking results and tracking error are displayed in Figure 15. As it is seen in Figure 15, the ship system can obtain good performance under the designed control law, and the tracking error of the system can be very small by selecting appropriate parameters. Moreover, the curves of states and control input are shown in Figures 16 and 17, respectively.

Note 7: Note that the size of the tracking error e_1 is affected by the designed parameters $c_i, \eta_i, \Phi_i, \tau_i, \pi_n$ and ϑ . Moreover, in the simulation analysis, for other parameters, such as $\varepsilon_1^*, \varepsilon_2^*$ and μ_3^* , are randomly selected, which increases the conservatism of the results to a certain extent. In order to reduce conservatism, we can improve the approximation ability

of fuzzy system to nonlinear dynamics by setting the initial value. We can also find the optimal parameters by introducing the optimization method.

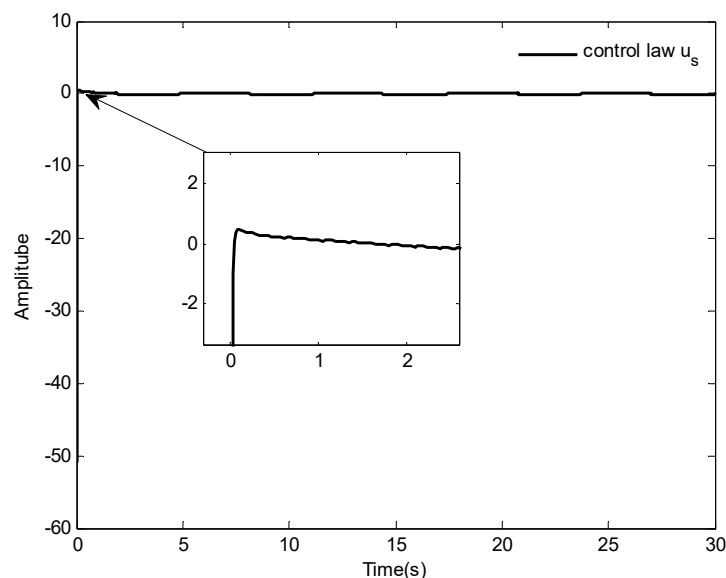


Figure 17. The curve of control input $u_s(t)$.

6. Conclusions

This paper discusses the tracking control problem of an uncertain nonlinear system with actuator faults by using the adaptive fuzzy control law. The fuzzy logic systems are considered to approximate the uncertain nonlinear functions, and then an adaptive fuzzy dynamic surface control law is proposed. Based on the dynamic surface control technique, the problem of the “explosion of complexity” can be overcome. The simulation results illustrate the effectiveness of the proposed control law. It has been proved that: (a) all of the signals in the closed-loop system are semi-global bounded, (b) the tracking error of the system can converge to a small neighborhood of the origin by adjusting the control law parameters, and (c) fairly good control performance is achieved despite the existence of the actuator fault and uncertain nonlinear dynamics in the system.

The extension of the proposed control law to more complex systems, such as pure-feedback systems and large-scale systems with input delays, is the direction of our future work. In addition, we will also focus on the command filter control method to solve the tracking control problem of system (1) with unknown control directions.

Author Contributions: Conceptualization, J.W. and X.D.; methodology, X.D.; software, J.W.; validation, J.W. and X.D.; formal analysis, X.D.; investigation, J.W. and X.D.; resources, X.D.; data curation, J.W.; writing—original draft preparation, X.D.; supervision, J.W. and X.D. All authors have read and agreed to the published version of the manuscript.

Funding: This research was supported by the Key Project of the Natural Science Research of Universities in Anhui Province under grant KJ2020A0344, and the Pre-research Project of the National Natural Science Foundation of Anhui Polytechnic University under grant Xjky2020020, and the Program for the Top Talents of Anhui Polytechnic University.

Institutional Review Board Statement: Not applicable.

Informed Consent Statement: Not applicable.

Data Availability Statement: Not applicable.

Conflicts of Interest: The authors declare no conflict of interest.

References

1. Zhang, B.Y.; Sun, X.X.; Liu, S.G.; Deng, X.F. Distributed fault tolerant model predictive control for multi-unmanned aerial vehicle system. *Asian J. Control* **2021**. [[CrossRef](#)]
2. Yoo, S.J.; Park, B.S. Quantized feedback control strategy for tracking performance guarantee of nonholonomic mobile robots with uncertain nonlinear dynamics. *Appl. Math. Comput.* **2021**, *407*, 126349. [[CrossRef](#)]
3. Cheng, X.; Zhang, Y.J.; Liu, H.S.; Wollherr, D.; Buss, M. Adaptive neural backstepping control for flexible-joint robot manipulator with bounded torque inputs. *Neurocomputing* **2021**, *458*, 70–86. [[CrossRef](#)]
4. Chen, Z.Y.; Yang, X.H.; Liu, X.P. RBFNN-based nonsingular fast terminal sliding mode control for robotic manipulators including actuator dynamics. *Neurocomputing* **2019**, *362*, 72–82. [[CrossRef](#)]
5. Zhang, R.D. Improved control for industrial systems over model uncertainty: A receding horizon expanded state space control. *IEEE Trans. Syst. Man Cybern. Syst.* **2020**, *50*, 1343–1349. [[CrossRef](#)]
6. Ji, R.H.; Ma, J.; Li, D.Y.; Ge, S.Z.S. Finite-time adaptive output feedback control for mimo nonlinear systems with actuator faults and saturations. *IEEE Trans. Fuzzy Syst.* **2021**, *29*, 2256–2270. [[CrossRef](#)]
7. Peng, J.Z.; Dubay, R. Adaptive fuzzy backstepping control for a class of uncertain nonlinear strict-feedback systems based on dynamic surface control approach. *Expert Syst. Appl.* **2019**, *120*, 239–252. [[CrossRef](#)]
8. Ling, S.; Wang, H.Q.; Liu, P.X.P. Fixed-time adaptive event-triggered tracking control of uncertain nonlinear systems. *Nonlinear Dyn.* **2020**, *100*, 3381–3397. [[CrossRef](#)]
9. Yang, Z.J.; Zhang, H.G. A fuzzy adaptive tracking control for a class of uncertain strict-feedback nonlinear systems with dead-zone input. *Neurocomputing* **2018**, *272*, 130–135. [[CrossRef](#)]
10. Wu, L.B.; Yang, G.H. Adaptive fuzzy tracking control for a class of uncertain nonaffine nonlinear systems with dead-zone inputs. *Fuzzy Sets Syst.* **2016**, *290*, 1–21. [[CrossRef](#)]
11. Jeong, D.M.; Yoo, S.J. Adaptive event-triggered tracking using nonlinear disturbance observer of arbitrarily switched uncertain nonlinear systems in pure-feedback form. *Appl. Math. Comput.* **2021**, *407*, 126335. [[CrossRef](#)]
12. Lin, W.; Wang, Y.J.; Liu, X.L. Asymptotic stabilization of nonlinear systems with long input delay via memoryless feedback: A linearization method. *Automatica* **2021**, *130*, 109731. [[CrossRef](#)]
13. Wang, F.; Liu, Z.; Zhang, Y.; Chen, C.L.P. Adaptive quantized fuzzy control of stochastic nonlinear systems with actuator dead-zone. *Inf. Sci.* **2016**, *370*, 385–401. [[CrossRef](#)]
14. Zhao, Y.; Liu, Y.F.; Wen, G.H.; Yu, X.H.; Chen, G.R. Distributed average tracking for lipschitz-type of nonlinear dynamical systems. *IEEE Trans. Cybern.* **2019**, *49*, 4140–4152. [[CrossRef](#)] [[PubMed](#)]
15. Deng, X.F.; Zhang, C.; Ge, Y. Adaptive neural network dynamic surface control of uncertain strict-feedback nonlinear systems with unknown control direction and unknown actuator fault. *J. Frankl. Inst.* **2022**. [[CrossRef](#)]
16. Shao, X.F.; Ye, D. Event-based adaptive fuzzy fixed-time control for nonlinear interconnected systems with non-affine nonlinear faults. *Fuzzy Sets Syst.* **2022**, *432*, 1–27. [[CrossRef](#)]
17. Wang, S.X.; Xia, J.W.; Wang, X.L.; Yang, W.J.; Wang, L.Q. Adaptive neural networks control for MIMO nonlinear systems with unmeasured states and unmodeled dynamics. *Appl. Math. Comput.* **2021**, *408*, 126369. [[CrossRef](#)]
18. Li, X.Y.; Wen, C.Y.; Zou, Y. Adaptive backstepping control for fractional-order nonlinear systems with external disturbance and uncertain parameters using smooth control. *IEEE Trans. Syst. Man Cybern. Syst.* **2021**, *51*, 7860–7869. [[CrossRef](#)]
19. Zhao, K.; Song, Y.D.; Chen, C.L.P.; Chen, L. Control of nonlinear systems under dynamic constraints: A unified barrier function-based approach. *Automatica* **2020**, *119*, 109102. [[CrossRef](#)]
20. Meng, F.F.; Zhao, L.; Yu, J.P. Backstepping based adaptive finite-time tracking control of manipulator systems with uncertain parameters and unknown backlash. *J. Frankl. Inst.* **2020**, *357*, 11281–11297. [[CrossRef](#)]
21. Parsa, P.; Akbarzadeh-T, M.R.; Baghbani, F. Command-filtered backstepping robust adaptive emotional control of strict-feedback nonlinear systems with mismatched uncertainties. *Inf. Sci.* **2021**, *579*, 434–453. [[CrossRef](#)]
22. Cui, G.Z.; Yu, J.P.; Wang, Q.G. Finite-time adaptive fuzzy control for mimo nonlinear systems with input saturation via improved command-filtered backstepping. *IEEE Trans. Syst. Man Cybern. Syst.* **2022**, *52*, 980–989. [[CrossRef](#)]
23. Wu, L.B.; Wang, H.; He, X.Q.; Zhang, D.Q. Decentralized adaptive fuzzy tracking control for a class of uncertain large-scale systems with actuator nonlinearities. *Appl. Math. Comput.* **2018**, *332*, 390–405. [[CrossRef](#)]
24. Dastres, H.; Rezaie, B.; Baigzadehnoe, B. Neural-network-based adaptive backstepping control for a class of unknown nonlinear time-delay systems with unknown input saturation. *Neurocomputing* **2020**, *398*, 131–152. [[CrossRef](#)]
25. Liu, H.; Pan, Y.P.; Cao, J.D.; Wang, H.X.; Zhou, Y. Adaptive neural network backstepping control of fractional-order nonlinear systems with actuator faults. *IEEE Trans. Neural Netw. Learn. Syst.* **2020**, *31*, 5166–5177. [[CrossRef](#)]
26. Ma, H.; Liang, H.J.; Zhou, Q.; Ahn, C.K. Adaptive dynamic surface control design for uncertain nonlinear strict-feedback systems with unknown control direction and disturbances. *IEEE Trans. Syst. Man Cybern. Syst.* **2019**, *49*, 506–515. [[CrossRef](#)]
27. Jia, F.J.; Yan, X.; Wang, X.H.; Lu, J.W.; Li, Y.M. Robust adaptive prescribed performance dynamic surface control for uncertain nonlinear pure-feedback systems. *J. Frankl. Inst.* **2020**, *357*, 2752–2772. [[CrossRef](#)]
28. Zhao, K.; Song, Y.D. Removing the feasibility conditions imposed on tracking control designs for state-constrained strict-feedback systems. *IEEE Trans. Autom. Control* **2019**, *64*, 1265–1272. [[CrossRef](#)]
29. Edalati, L.; Sedigh, A.K.; Shooredeli, M.A.; Moarefianpour, A. Adaptive fuzzy dynamic surface control of nonlinear systems with input saturation and time-varying output constraints. *Mech. Syst. Signal Processing* **2018**, *100*, 311–329. [[CrossRef](#)]

30. Rahmani, Z.; Baigzadehnoe, B.; Rezaie, B. Tracking control of a class of nonlinear systems with output delay based on adaptive fuzzy dynamic surface control. *Int. J. Syst. Sci.* **2020**, *51*, 1280–1306. [[CrossRef](#)]
31. Baigzadehnoe, B.; Rahmani, Z.; Khosravi, A.; Rezaie, B. Adaptive decentralized fuzzy output feedback tracking control for a class of nonlinear large-scale systems with input delays. *Trans. Inst. Meas. Control* **2018**, *40*, 3534–3548. [[CrossRef](#)]
32. Baigzadehnoe, B.; Rahmani, Z.; Khosravi, A.; Rezaie, B. Adaptive decentralized fuzzy dynamic surface control scheme for a class of nonlinear large-scale systems with input and interconnection delays. *Eur. J. Control* **2020**, *54*, 33–48. [[CrossRef](#)]
33. Baigzadehnoe, B.; Rahmani, Z.; Khosravi, A.; Rezaie, B. Control of interconnected systems with sensor delay based on decentralized adaptive neural dynamic surface method. *J. Syst. Control Eng.* **2021**, *235*, 751–768.
34. Zhou, Z.Y.; Tong, D.B.; Chen, Q.Y.; Zhou, W.N.; Xu, Y.H. Adaptive NN control for nonlinear systems with uncertainty based on dynamic surface control. *Neurocomputing* **2021**, *421*, 161–172. [[CrossRef](#)]
35. Song, S.; Zhang, B.Y.; Song, X.N.; Zhang, Z.Q. Adaptive neuro-fuzzy backstepping dynamic surface control for uncertain fractional-order nonlinear systems. *Neurocomputing* **2019**, *360*, 172–184. [[CrossRef](#)]
36. Shao, X.F.; Ye, D. Fuzzy adaptive event-triggered secure control for stochastic nonlinear high-order mass subject to DoS attacks and actuator faults. *IEEE Trans. Fuzzy Syst.* **2021**, *29*, 3812–3821. [[CrossRef](#)]
37. Lv, M.L.; Yu, W.W.; Baldi, S. The set-invariance paradigm in fuzzy adaptive DSC design of large-scale nonlinear input-constrained systems. *IEEE Trans. Syst. Man Cybern. Syst.* **2021**, *51*, 1035–1045. [[CrossRef](#)]
38. Shojaei, F.; Arefi, M.M.; Khayatian, A.; Karimi, H.R. Observer-based fuzzy adaptive dynamic surface control of uncertain nonstrict feedback systems with unknown control direction and unknown dead-zone. *IEEE Trans. Syst. Man Cybern. Syst.* **2019**, *49*, 2340–2351. [[CrossRef](#)]
39. Wang, H.Q.; Liu, P.X.P.; Zhao, X.D.; Liu, X.P. Adaptive fuzzy finite-time control of nonlinear systems with actuator faults. *IEEE Trans. Cybern.* **2020**, *50*, 1786–1797. [[CrossRef](#)]
40. Zhao, K.J.; Chen, W. Adaptive neural quantized control of MIMO nonlinear systems under actuation faults and time-varying output constraints. *IEEE Trans. Neural Netw. Learn. Syst.* **2020**, *31*, 3471–3481. [[CrossRef](#)]
41. Ma, J.L.; Park, J.H.; Xu, S.Y. Global adaptive control for uncertain nonlinear systems with sensor and actuator faults. *IEEE Trans. Syst. Man Cybern. Syst.* **2021**, *51*, 5503–5510. [[CrossRef](#)]
42. Wang, Z.; Shan, J.J. Fixed-time consensus for uncertain multi-agent systems with actuator faults. *J. Frankl. Inst.* **2020**, *357*, 1199–1220. [[CrossRef](#)]
43. Wang, D.; Huang, J. Neural network-based adaptive dynamic surface control for a class of uncertain nonlinear systems in strict-feedback form. *IEEE Trans. Neural Netw.* **2005**, *16*, 195–202. [[CrossRef](#)]
44. Fortuna, L.; Muscato, G. A roll stabilization system for a monohull ship: Modeling, identification, and adaptive control. *IEEE Trans. Control Syst. Technol.* **1996**, *4*, 18–28. [[CrossRef](#)]